Extreme Mechanics Letters 57 (2022) 101913

Contents lists available at ScienceDirect

Extreme Mechanics Letters

journal homepage: www.elsevier.com/locate/eml

Understanding the mechanisms of adhesive wear for heterogeneous materials through atomistic simulations

S.Z. Wattel *, J. Garcia-Suarez, J.-F. Molinari

Civil Engineering Institute, Materials Science and Engineering Institute, Ecole Polytechnique Fédérale de Lausanne (EPFL), Switzerland

ARTICLE INFO

Article history:
Received 17 June 2022
Received in revised form 27 September 2022
Accepted 18 October 2022
Available online 26 October 2022

Keywords:
Adhesive wear
Molecular dynamics simulation
High-entropy composite
Homogenization

ABSTRACT

When two rough surfaces slide against each other, two main behaviors can be observed at the asperity level: A ductile behavior where the asperities tend to smooth out or a brittle behavior where the asperities detach and form debris. Recently, a critical length scale controlling the transition between both behaviors was identified. Its formulation depends only on material properties and a geometrical factor (of the order of unity). This finding was achieved thanks to molecular dynamics (MD) simulations with hardness-tunable interatomic potentials. However, the materials studied so far have been homogeneous. Here, the work is extended to a class of simple heterogeneous materials with random fluctuations of their properties. A comparative study of the heterogeneous materials against an equivalent homogeneous material is conducted to study the influence of the local variations on the global behavior. It is found that the critical junction size formula works well for hard materials up until a certain ductility threshold after which a third behavior, mixing shear localization and mode II crack opening, appears. There is a transition zone, larger for the heterogeneous material, from the ductile to the brittle behaviors due to local fluctuations and non-deterministic nature of finite temperature atomistic simulations. Local fluctuations render the heterogeneous material weaker than the equivalent homogeneous material and thus, following the critical junction size formula, should lower the probability of forming debris. While this effect can be observed in the single asperity simulations, its magnitude is lower than expected, hinting at the dichotomic effect of local variations: while they increase the overall ductility, they also create particularly brittle areas prone to crack nucleation.

1. Introduction

Tribology is the science of contacting surfaces in relative motion: it is the study of friction and wear. Tribological processes are omnipresent in the modern world, in fact frictional losses and replacement of worn parts are estimated to represent 23% of the global energy expenditure [1]. It is thus critically important to understand and to be able to predict wear and friction. However, most models are phenomenological in nature and use empirical parameters to fit experimental results [2]. One reason for this is the complexity of the physics and chemistry involved, as tribological processes mix solid and fluid mechanics, material science and roughness over several scales. Another factor is the difficulty to observe tribological processes in real time, as the sliding has to be stopped to observe the surfaces.

Simulation of tribological processes can give a glimpse of the mechanical phenomenon that the experimentalist eye cannot yet reach. For adhesive wear, which happens when both surfaces are of similar hardness and have significant adhesive forces between them, two basic competing views co-exist on the mechanisms at the asperity scale. On the one hand, Holm [3] suggested that wear happens by plastic deformation of the asperities, resulting in a smoothing process. This has been observed both in experiments [4–8] and in atomistic simulations [8–10]. However, this does not explain the formation of debris (sometimes called third body or gouge depending on the field) at the interface. Also, by taking this idea to its logical end, the two surfaces should cold weld after sufficient sliding, which does not happen systematically. More often, a steady-state of friction is reached [11].

On the other hand, Archard [12] explained adhesive wear by the fracture-induced detachment of the asperities that then form debris. This has been observed in experiments [13–16]. However, up until recently, simulations did not manage to reproduce the formation of debris.

An atomistic model devised in Ref. [17] captured for the first time both mechanisms in a single model by using a family of potential with tunable hardness. Thanks to this model, a critical length scale dictating the transition from one mechanism to the

* Corresponding author.
E-mail address: sacha.wattel@epfl.ch (S.Z. Wattel).

https://doi.org/10.1016/j.eml.2022.101913

other was found, as detailed in the next paragraph. Building on this work, other notable results were attained: the emergence of self-affine roughness in simulation similar to the one observed in nature [18], a new formula for wear rate from first principles [19] or a possible explanation for the transition from mild to severe wear at a critical load [20].

Critical junction size When asperities touch, they do so over an area that we call junction. By varying the size of the junction while keeping the material properties constant, it was found that large junctions lead to a behavior similar to Archard model whereas smaller junctions lead to a behavior closer to Holm predictions. An energy argument has been put forward and was verified numerically: a debris is formed when the stored elastic energy becomes larger than the energy necessary to create a crack and detach the asperity [11,17]. This led to the formulation of a critical junction size d^* only from material properties and a geometric parameter as:

$$d^* = \lambda \frac{2\gamma_{surf} G}{\tau_{el}^2}, \tag{1}$$

where γ_{surf} is the surface energy, G is the shear modulus, τ_{el} the elastic shear strength and λ is a geometry factor capturing the shape of the asperity, the path of the fracture and the area plastified (of the order of unity [17,20]).

This critical junction size provides an explanation for discrepant results where some experiments lead to a gradual smoothing [4,6,7,16,21–24] and others to debris formation [15,16,25].

However, the atomistic simulation of critical junction size and related wear topics [17,19,20,26] considered homogeneous materials. Completely homogeneous materials are rare in nature and heterogeneities, such as porosity, grain structure or inclusions, are often to be found. These heterogeneities create local fluctuations of mechanical properties and can greatly influence the global behavior. Here, we propose to extend the study of the critical junction size to a simple type of heterogeneous material, through the use of atomistic simulations. The range of possible heterogeneous patterns is large and thus a simple heterogeneous material is devised for this study: a bi-material *high-entropy composite*, where the two components are well mixed [27]. The insights acquired from the study of this material can then serve as a baseline for more complex composites.

2. Methods

All simulations are run using the MD software LAMMPS [28] and are constrained to be two-dimensional in space. Unless otherwise mentioned, all units are rendered dimensionless (reduced units) by taking a reference energy ϵ_0, length r_0 (respectively the depth and distance of the potential well) and atomic mass m_0 as well as a unity Boltzmann constant $k_B = 1$. The resulting reductions are summarized in Table 1.

Tunable model potentials Interatomic pair potentials whose inelastic properties can be tuned are used in this work [29]. The tail part of the potential can be modified without changing the energy well, implying that the plastic properties (strength, hardness, etc.) can be changed without affecting the elastic ones (stiffness, equilibrium lattice spacing, surface energy, etc.). The use of such potentials has proven to be an essential tool to reproduce brittle debris formation at computationally-affordable scales [17,19,29].

The potential energy can be expressed as:

$$\frac{V(r)}{\epsilon_0} = \begin{cases} (1-e^{\alpha(r-r_0)})^2 - 1 & r < 1.1r_0, \\ c_1\frac{r^3}{6} + c_2\frac{r^2}{2} + c_3 r + c_4 & 1.1r_0 \le r \le r_{cut}, \\ 0 & r_{cut} \le r, \end{cases} \tag{2}$$

where r is the interatomic distance, ϵ_0 the depth of the well, r_0 the interatomic distance of the bottom of the well and $\alpha = 3.93\, r_0^{-1}$ is a parameter that tunes the stiffness. The tail of the potential can be shortened or elongated with r_{cut}, the parameters c_1, c_2, c_3 and c_4 are chosen to ensure continuity of the potential and its derivative at $r = 1.1r_0$ and $r = r_{cut}$.

High-entropy composite Since the short-range interaction between atoms does not vary when the ductility is tuned, the equilibrium lattice spacing also remains the same, meaning that "brittle" and "ductile" atoms can be used interchangeably in a lattice at equilibrium without affecting the lattice structure or creating internal stress. We make use of this property to create a so-called *high-entropy composite*: starting from a grid of *brittle atoms*, a random fraction f is replaced by *ductile atoms*, as illustrated in Fig. 1a. Three pair potentials, whose profiles are drawn in Fig. 1a, are used: a short-tailed brittle one, P_b ($r_{cut} = 1.42\, r_0$), between *brittle atoms*, a long-tailed ductile one, P_d ($r_{cut} = 1.71\, r_0$), between *ductile atoms* and an intermediate one, P_m ($r_{cut} = 1.56\, r_0$), between *brittle* and *ductile atoms*. The lower limit of r_{cut} was chosen so that ductile behavior could still be observed for very small junction size of a few atoms but quickly transitioned to brittle behaviors. For the upper limit of r_{cut}, the transition happens at a computationally affordable scale of around 100 to 200 atoms.

Equivalent homogeneous material The stochastic nature of the creation of the high-entropy composite will lead to local fluctuations in the distribution of the *ductile* and *brittle atoms*, and thus spatial fluctuations of the mechanical properties. While at larger scale, some properties of the composite (such as stiffness) are expected to homogenize well, some might depend heavily on these local variations. For example, the presence of a cluster of brittle atoms around a point of stress concentration could lead to the earlier formation of a crack and a global brittle behavior in a case where ductile behavior would have been expected if only the homogenized properties had been regarded. To quantify this *local effect*, an equivalent homogeneous material can be defined, using a single average-atom pair potential P_h between all atoms [27]. This equivalent material has, for example, the same stacking fault energy in average. Then, the differences between the homogenized material and the composite can be interpreted as a measure of the influence of *local effects*. The equivalent potential P_h can be found with the following expression adapted from Ref. [27]:

$$P_h(f) = (1-f)^2 P_b + 2f(1-f)P_m + f^2 P_d, \tag{3}$$

with f the fraction of ductile atoms that would be in the high-entropy composite. The terms f^2, $f(1-f)$ and $(1-f)^2$ are the proportions of bonds using the ductile, medium and brittle pair potentials, respectively.

Shear strength Three material parameters appear in the critical junction size formula Eq. (1). On the one hand, the surface energy and the tangent shear modulus at small strain are dependent on the short range interactions of the interatomic potentials. Thus, in our case, they are independent of the fraction of ductile atoms f for both the homogeneous material and the composite. On the other hand, the shear strength is highly dependent on the tail part of the potentials and thus is expected to vary with f. Thus, it would be useful to know the dependence of the shear strength on f to verify if the prediction of critical junction size applies to heterogeneous materials. However, at the atomic scale, the meaning of shear strength is not well-defined, and is dependent on the crystalline structure. In this paper, we focus on the shear strength along a slip plane of the hexagonal lattice. The most-constrained measurement is with the GSF (Generalized Stacking Fault) curve whose maximum derivative gives the ideal shear strength [31,32]. Here, the movement parallel to the shearing is

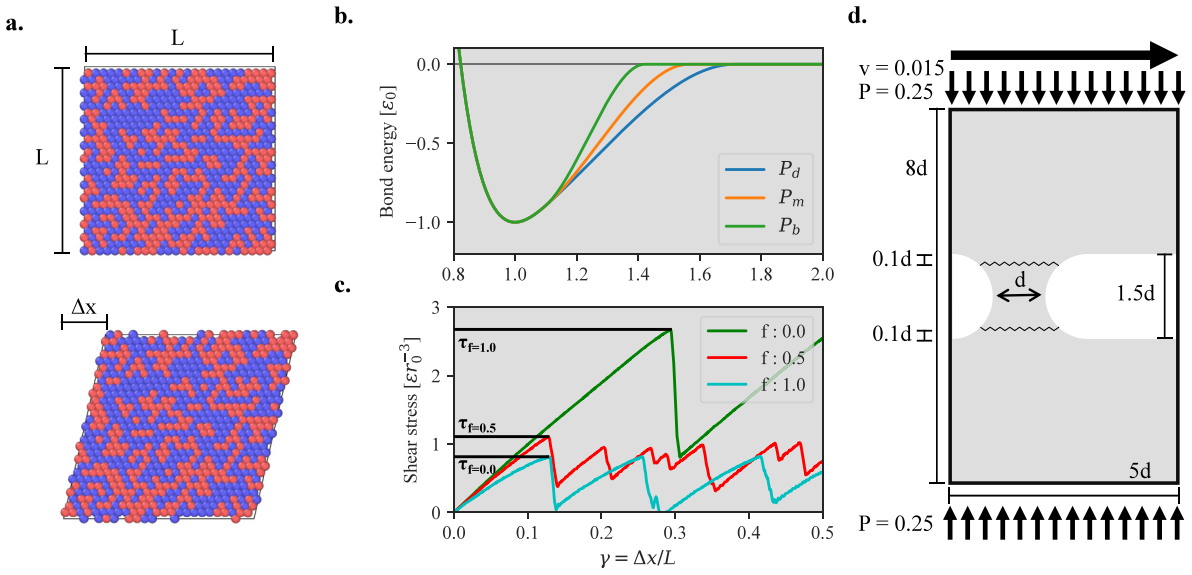

Fig. 1. a. Square box of composite material, initial state on top, deformed on the bottom. The red atoms are linked to the brittle potential, the blue ones to the ductile. Atomistic simulations snapshots made with OVITO [30]. **b.** Profiles of the three interatomic potentials used for the high-entropy composite material. **c.** Typical shear simulation results with the volume-averaged virial shear stress as a function of the shear strain for three different fractions of ductile atoms f. In black, the considered shear strengths. **d.** Domain and boundary conditions of contacting asperities simulations. The jagged lines correspond to the assumed crack paths for the calculation of the geometric factor λ in the critical junction size formula [Eq. (1)]. (All quantities in reduced units as summarized in Table 1). (For interpretation of the references to color in this figure legend, the reader is referred to the web version of this article.)

Table 1
Table of reductions used to render all quantities dimensionless. These reductions are common within the atomistic simulation community and are sometimes referred to as Lennard-Jones reduced unit. k_B is the Boltzmann constant.

Quantity	Reduction
Distance	r_0
Mass	m_0
Energy	ϵ_0
Time	$r_0\sqrt{m_0\epsilon_0^{-1}}$
Velocity	$\sqrt{m_0^{-1}\epsilon_0}$
Force	$\epsilon_0 r_0^{-1}$
Pressure	$\epsilon_0 r_0^{-3}$
Temperature	$\epsilon_0 k_B^{-1}$
Shear rate	$r_0^{-1}\sqrt{m_0^{-1}\epsilon_0}$

totally constrained. The equivalent homogeneous material has the same GSF curve as the composite in average, over realizations or for a box large enough. Thus, both materials have the same ideal shear strength. However, local variations present in the composite may have an effect on other measurements of the shear strength. The approach chosen for this work to evaluate shear strength is slightly less constrained than the GSF curve: a square box with periodic boundaries is sheared and the maximum volume averaged virial stress attained is picked as the shear strength as represented in Fig. 1a and b. Here, local variations present in the composite are expected to have an impact on the measurements and the behavior of the composite and the equivalent homogeneous material should diverge. To find the dependence of the shear strength on f, the shear strengths of both the composite and equivalent uniform material were measured for different fractions f of ductile atoms. The size was varied until convergence was observed to catch *size effects*. As the results depend on the initial configurations, 30 realizations of each fraction and size were run. The box is populated with atoms on a hexagonal lattice, with a lattice constant corresponding to the equilibrium one at a temperature of 0.025. Initial velocities are distributed at random and scaled so that the initial temperature is 0.05. The box is deformed at a shear rate of 0.001 and the time integration is solved via a NVT scheme with a Nose–Hoover thermostat [33,34] set at 0.025 and with a time step of 0.005. The shearing is parallel to a weak plane of the lattice. The resulting stress considered is the overall virial stress. The size of the box is a multiple of the lattice constant to avoid initial tension at the parallel boundaries. From these simulations, both the shear modulus and the shear strength can be determined: the shear strength is the maximal shear volume-averaged virial stress attained (see Fig. 1b) and the shear modulus is taken as the slope between the origin and the stress at 0.5% shear deformation.

Single asperity simulation To investigate how the composite behaves in an adhesive wear scenario, sliding simulations where each surface has a single asperity can be used. The asperities collide and may either smooth out plastically or detach, creating rolling debris. Compared to rough surfaces sliding simulations, they allow an easier control of the asperity shape and contact junction size. Here, another type of simulation is used: we start with two surfaces connected by a bridge of minimum width d as represented in Fig. 1c. The bridge represents two asperities already in contact so as to readily control the junction size and to facilitate the post-processing. This simplification has been validated in previous work [35,36] to have little effect on the outcome. The goal is to identify if the bridge detaches and forms a rolling third body or if it plastically crushes out when a sliding motion is applied. For each fraction f, different junction sizes are tested in order to catch the transition from one behavior to the other. A normal pressure $P = 0.25$ is applied to the top and bottom boundaries, the bottom row of atoms is held in place horizontally and a horizontal velocity $v = 0.015$ is imposed on the top row. This velocity is small enough to rule out dynamical effects. The left and right boundary conditions are periodic.

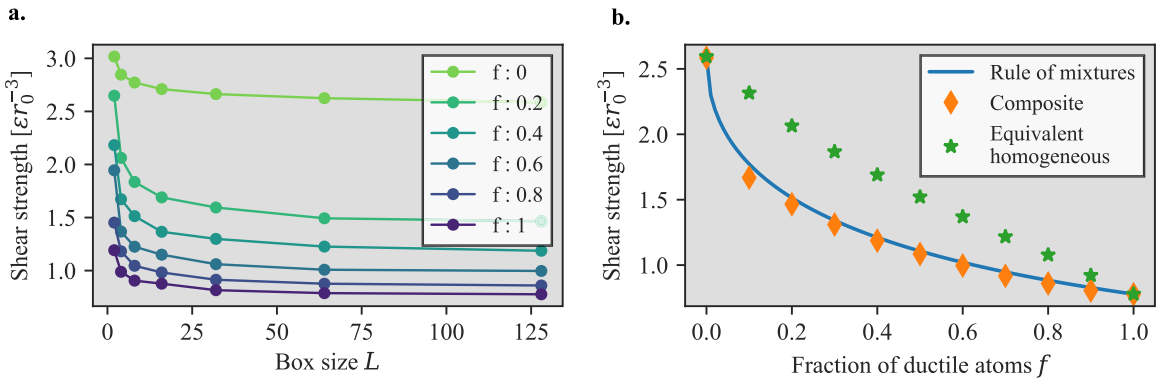

Fig. 2. **a.** Shear strength of the high-entropy composite for different box size L. **b.** Shear strength of the high-entropy composite and equivalent homogeneous material at different fraction f, averaged over 30 realizations. Also plotted is the rule of mixture (Eq. (5)) that matches well the ones of the composite.

The atoms are arranged in a hexagonal lattice, with a lattice constant corresponding to the equilibrium one at a temperature of $T = 0.025$. Initial velocities are distributed at random and scaled so that the initial temperature is 0.05. A six-atom-thick bulk-velocity-corrected Langevin thermostat [37] is present on the top and bottom, set at $T = 0.025$. The time-integration is done through a Verlet algorithm with a timestep of 0.005.

Critical junction size As the shear strength can be dependent on the length scale considered, the definition of d^* is implicit:

$$d^* = \lambda \frac{2\gamma_{surf} G}{\tau_{el}^2(d^*, f)}. \tag{4}$$

For each fraction f, d^* was found thanks to a fixed-point iteration algorithm. As the shear strength is known only for the specific box sizes d at which it was measured, a linear interpolation was used to estimate the shear strength between those box sizes.

The geometric pre-factor λ corresponds to, in the two-dimensional case, the ratio of the total length of the cracks necessary to detach the asperity to the plastically sheared area (in 3D, it is volume and area respectively). For the specific geometry used, the pre-factor is $\lambda = 1.35$ considering horizontal cracks close to the base of the bridge (as shown in Fig. 1c) and the area between the cracks completely plastified.

3. Results

3.1. Shear strength

Size effect There is a strengthening effect with diminishing box sizes, as shown in Fig. 2. The strengthening is only observable for smaller box and plateaus to a finite value for larger box. This effect is expected when heterogeneity is present, as a smaller domain is less likely to have *weak spots* (such as a large cluster of ductile atoms). If these defects have a greater than linear effect, then the overall strength of larger samples is lower. A useful analogy for this behavior is a chain, which is as strong as its weakest link: larger chains have a higher likeliness of having a weak link and thus are weaker in average. In another view, this effect could be compared to Hall–Petch strengthening [38,39] for poly-crystalline materials, which consists in an increase in the strength of the material with the inverse of the square root of the grain size.

Rule of mixture In Fig. 2, both the shear strength of the composite and the homogeneous material for the largest box[1] as a function of the fraction of ductile atoms are plotted. While the shear strength of the equivalent homogeneous displays an almost linear relationship with the fraction, the strength of the composite is lower. A new formulation for the rule of mixture was found to match well the numerical results. It relates the ratio of the strength of the pure components to the one of the composite as such:

$$\frac{\tau(f)}{\tau_d} = \left(\frac{\tau_b}{\tau_d}\right)^{f^A}, \tag{5}$$

with $\tau(f)$, τ_d and τ_b the shear strengths of the composite at fraction f, of the pure ductile and pure brittle materials respectively. The only empirical constant is $A = 0.5 \pm 0.05$, depending on the box size. The almost-square-root exponent arises from the fitting, we have not found a first principal explanation thereof.

The gap in strength between the high-entropy composite and the equivalent homogenized material is attributed to *local effects*. Indeed, in the composite, there may be clumps of ductile atoms, which display lower shear strength: a dislocation is more likely to initiate in these areas and then lead to lower global shear strength. The composite with a fraction of ductile atoms close to 0.5 are more heterogeneous than the one with f close to zero or one, they have more defects and thus the gap in shear strength with the equivalent homogeneous material is larger.

3.2. Debris creation

Global behavior The contacting asperities simulations resulted in three distinct behaviors. For low-ductility simulations, up to a fraction of ductile atoms of $f = 0.7$, the behaviors observed are similar to previous work [17]: for large junction sizes and more brittle material, the outcome will be a debris-inducing behavior with tensile cracks opening on the base of the asperities (Fig. 3 top) whereas the behavior will be ductile and results in a smoothing of the surfaces and eventually cold-welding for a smaller junction size and more ductile material (Fig. 3 middle). For high-ductility simulations, a third behavior appears: plastic shearing concentrates at the base of the asperities and cracks open through in-plane shearing on either or both bases of the asperities. The vertical pressure closes the horizontal crack eventually and thus prevents debris-creation. When no vertical pressure is applied, the asperity does detach. It should be noted that the atoms are arranged in a hexagonal lattice with a slip plane parallel to the shearing motion, thus facilitating this behavior.

Transition zone Even with a fixed geometry and homogeneous material, the outcome of the simulations is stochastic in

[1] Where the small size strengthening effect can be neglected.

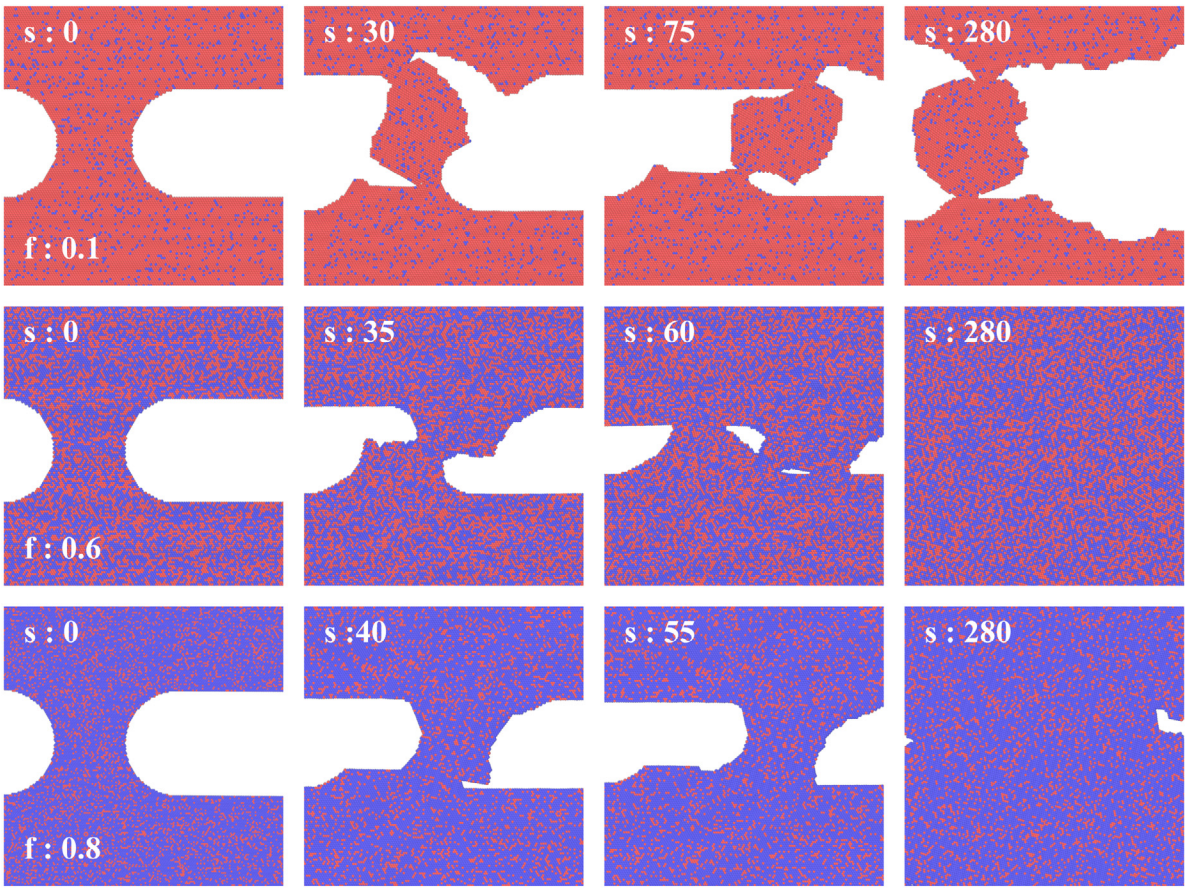

Fig. 3. Snapshots of simulations at increasing sliding distances s, evidencing the three outlined behaviors: brittle and debris-forming on top, ductile and smoothing in the middle and mix in the bottom. All the simulations have the same junction size $d = 30$. The red atoms are linked to the brittle potential, the blue ones to the ductile. The sliding distance s and the fraction of ductile atoms f in the annotation. Atomistic simulations snapshots made with OVITO [30]. (For interpretation of the references to color in this figure legend, the reader is referred to the web version of this article.)

nature because of the initial random velocity distribution due to the finite temperature. For high-entropy composite, it is even more stochastic. Thus, for each configuration (junction size d and fraction of ductile atoms f), the simulations were run for five realizations. Focusing on the low ductility simulations ($f < 0.7$), the results were split in two categories depending on whether a rolling third body was present at the end of the simulation. In Fig. 4, there is a point for each configuration and the shade of blue to yellow represents the part of realizations where roller debris are observed. For both the composite and the homogeneous materials, two zones clearly appear in the $f - d$ plane: for higher ductility and small junction size, the bridge smooths out whereas a third body is formed for higher junction size and lower ductility. These two zones are separated by a transition zone. To better capture the transition, 40 realizations at $f = 0.5$ and for varying junction sizes were run for both materials, the results are plotted in Fig. 5. The transition has an S-curve shape, starting at zero (meaning no debris creation) for small junction size and going to one for higher junction size (meaning that a rolling third body was observed in all simulations). This fraction from zero to one can be interpreted as the probability to observe debris creation in a realization at a given junction size d. In other words, it is the probability $P(d^* < d)$ that the critical junction size d^* is lower than d: in this view, the S-curve is a cumulative density function of the random variable d^*. By assuming that d^* is drawn from a normal law, which is a good fit to the data, we can obtain the mean critical junction size $\bar{d}$ as well as its standard deviation SD (indicative of the size of the transition zone) from the distribution:

$$P(d^* < d) = \int_{-\infty}^{d} \frac{1}{SD\sqrt{2\pi}} e^{-0.5\left(\frac{x-\bar{d}}{SD}\right)^2} dx. \tag{6}$$

As expected, the transition zone for the composite material ($SD_{comp} = 8.4$) is greater than the one for the homogeneous material ($SD_{equi} = 5.0$) as the random local fluctuations of the composite create a greater range for variations between realizations.

Critical junction size From the shear strengths measured before, it is possible to compute, for both the composite and homogeneous material, the predictions of the critical junction size formula, as plotted in Fig. 4. For the homogeneous material, there is a good agreement between the simulation results and the predicted critical junction size: the curve falls in the transition zone. For the composite, according to the critical junction size formula, the lower measured shear strength should lead to a more ductile behavior than the homogeneous material. While this is indeed reflected in the results, the effect is not as strong as expected and the critical junction size of the composite falls between both predictions. This points at the existence of a brittle mechanism caused by local variation of the hardness: the presence of brittle patches may favor an early crack initiation, leading to a more brittle global behavior.

4. Conclusion

The comparative study of the heterogeneous material and the equivalent homogenized one has yielded several salient results. First, a simple homogenization scheme is not sufficient to capture

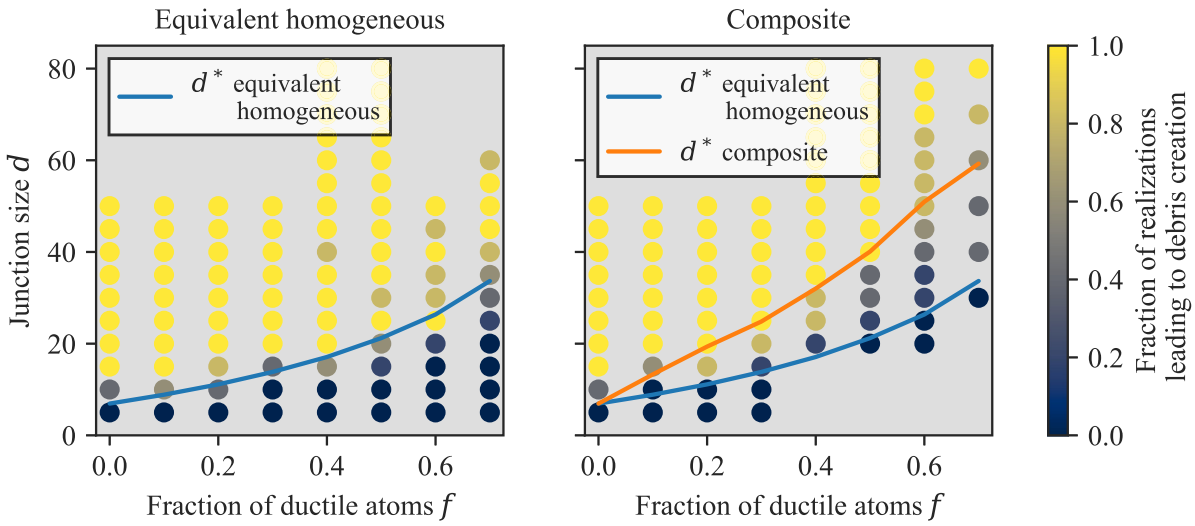

Fig. 4. Results of single asperity sliding simulations, **a.** Equivalent homogeneous material and **b.** High-entropy composite. Each point represents five realizations at a given fraction of ductile atoms f and junction size d, the shade from blue to yellow gives the proportion of simulations that lead to debris creation, as indicated by the legend on the right. The blue line corresponds to the critical junction size d^* calculated with the shear strength of the equivalent homogeneous material, the green line with the shear strength of the composite. (For interpretation of the references to color in this figure legend, the reader is referred to the web version of this article.)

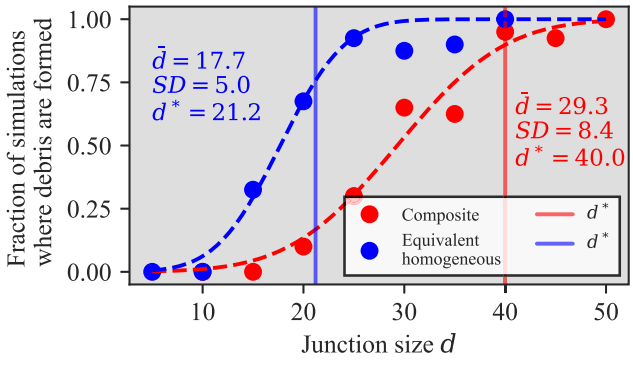

Fig. 5. Fraction of simulations that lead to debris creation out of 40 realizations for a fraction of ductile atoms $f = 0.5$, for both the composite and homogeneous equivalent material. The dashed lines are the cumulative density functions of the normal law fitted to the data, with the mean $\bar{d}$ and standard deviation SD in the annotation. The vertical lines correspond to the prediction of the critical junction size formula (Eq. (1)) for the composite and homogeneous material.

the effect of local variations, at any scale. Indeed, even though the two materials studied have the same GSF curve in average and thus the same ideal shear strength, the high-entropy composite appears weaker when tested with other methods of shear strength measurement. The occurrence of clusters of *ductile atoms* in the composite favors the onset of dislocations and thus reduces non-linearly the overall shear strength.

Following the critical junction size formula, the lower shear strength should lead, all else being equal, to a more ductile behavior in adhesive wear scenarii. While such an effect has been observed, the composite is not as ductile as predicted. This could be explained by particularly brittle spots offering ideal conditions for crack nucleation. Once a crack has opened, the probability of global brittle behavior is increased. Thus, both brittle and ductile spots influence the global behavior.

A new behavior of asperity yielding, mixing large plasticity and mode II crack opening was uncovered for highly ductile materials. In this case, the critical junction size fails to appropriately predict the behavior.

Finally, while the family of heterogeneous materials studied here is simple, its stochastic nature leads to complex results. It highlights that the critical junction size d^* cannot be interpreted as a deterministic rule. Rather, it can be seen as the mean of a probabilistic distribution describing the chance of forming debris and resulting in a S-curve-shaped transition zone between ductile and brittle behavior. The design space of the high-entropy composite described here depends on only a single bounded parameter (the fraction of ductile atoms f). This allows running parametric studies without dimensionality issues. No explicit assumptions were made on the structure or scale of the heterogeneities, making it an ideal baseline model for the study of more structured composites.

Declaration of competing interest

The authors declare that they have no known competing financial interests or personal relationships that could have appeared to influence the work reported in this paper.

Data availability

The scripts are uploaded on Zenodo: https://doi.org/10.5281/zenodo.6657120.

Acknowledgments

This work was supported by the Swiss National Science Foundation under the grant “Wear across scales” (197152). The authors thank William A. Curtin for providing helpful discussion on the average-atom interatomic potential for building the equivalent homogeneous material.

References

[1] K. Holmberg, A. Erdemir, Influence of tribology on global energy consumption, costs and emissions, Friction 5 (3) (2017) 263–284.
[2] H.C. Meng, K.C. Ludema, Wear models and predictive equations: Their form and content, Wear 181–183 (1995) 443–457.

[3] R. Holm, Electric Contacts: Theory and Application, Springer, Berlin, Heidelberg, 1967.
[4] B. Gotsmann, M.A. Lantz, Atomistic Wear in a Single Asperity Sliding Contact, Phys. Rev. Lett. 101 (12) (2008) 125501, Publisher: American Physical Society.
[5] H. Bhaskaran, B. Gotsmann, A. Sebastian, U. Drechsler, M.A. Lantz, M. Despont, P. Jaroenapibal, R.W. Carpick, Y. Chen, K. Sridharan, Ultralow nanoscale wear through atom-by-atom attrition in silicon-containing diamond-like carbon, Nature Nanotechnol. 5 (3) (2010) 181–185.
[6] T. Sato, T. Ishida, L. Jalabert, H. Fujita, Real-time transmission electron microscope observation of nanofriction at a single Ag asperity, Nanotechnology 23 (50) (2012) 505701, Publisher: IOP Publishing.
[7] T.D.B. Jacobs, R.W. Carpick, Nanoscale wear as a stress-assisted chemical reaction, Nature Nanotechnol. 8 (2) (2013) 108–112.
[8] P. Stoyanov, P.A. Romero, R. Merz, M. Kopnarski, M. Stricker, P. Stemmer, M. Dienwiebel, M. Moseler, Nanoscale sliding friction phenomena at the interface of diamond-like carbon and tungsten, Acta Mater. 67 (2014) 395–408.
[9] M.R. Sorensen, K.W. Jacobsen, P. Stoltze, Simulations of atomic-scale sliding friction, Phys. Rev. B 53 (4) (1996) 2101–2113, Publisher: American Physical Society.
[10] J. Zhong, R. Shakiba, J.B. Adams, Molecular dynamics simulation of severe adhesive wear on a rough aluminum substrate, J. Phys. D: Appl. Phys. 46 (5) (2013) 055307, Publisher: IOP Publishing.
[11] E. Rabinowicz, Friction and Wear of Materials, Wiley, New York, 1995.
[12] J.F. Archard, Contact and Rubbing of Flat Surfaces, J. Appl. Phys. 24 (8) (1953) 981–988, Publisher: American Institute of Physics.
[13] J.A. Greenwood, D. Tabor, Deformation Properties of Friction Junctions, Proc. Phys. Soc. B 68 (9) (1955) 609–619, Publisher: IOP Publishing.
[14] C.A. Brockley, G.K. Fleming, A model junction study of severe metallic wear, Wear 8 (5) (1965) 374–380.
[15] K.-H. Chung, D.-E. Kim, Fundamental Investigation of Micro Wear Rate Using an Atomic Force Microscope, Tribol. Lett. 15 (2) (2003) 135–144.
[16] J. Liu, J.K. Notbohm, R.W. Carpick, K.T. Turner, Method for Characterizing Nanoscale Wear of Atomic Force Microscope Tips, ACS Nano 4 (7) (2010) 3763–3772, Publisher: American Chemical Society.
[17] R. Aghababaei, D.H. Warner, J.-F. Molinari, Critical length scale controls adhesive wear mechanisms, Nature Commun. 7 (1) (2016) 11816.
[18] E. Milanese, T. Brink, R. Aghababaei, J.-F. Molinari, Emergence of self-affine surfaces during adhesive wear, Nature Commun. (2019).
[19] R. Aghababaei, D.H. Warner, J.-F. Molinari, On the debris-level origins of adhesive wear, Proc. Natl. Acad. Sci. (2017) Num Pages: 6 Place: Washington Publisher: Natl Acad Sciences.
[20] R. Aghababaei, T. Brink, J.-F. Molinari, Asperity-Level Origins of Transition from Mild to Severe Wear, Phys. Rev. Lett. (2018).
[21] Z. Tao, B. Bhushan, Surface modification of AFM silicon probes for adhesion and wear reduction, Tribol. Lett. 21 (1) (2006) 1.
[22] A.P. Merkle, L.D. Marks, Liquid-like tribology of gold studied by in situ TEM, Wear 265 (11) (2008) 1864–1869.
[23] V. Vahdat, D.S. Grierson, K.T. Turner, R.W. Carpick, Mechanics of Interaction and Atomic-Scale Wear of Amplitude Modulation Atomic Force Microscopy Probes, ACS Nano 7 (4) (2013) 3221–3235, Publisher: American Chemical Society.
[24] K.-H. Chung, Wear characteristics of atomic force microscopy tips: A review, Int. J. Precis. Eng. Manuf. 15 (10) (2014) 2219–2230.
[25] B. Bhushan, S. Sundararajan, Micro/nanoscale friction and wear mechanisms of thin films using atomic force and friction force microscopy, Acta Mater. 46 (11) (1998) 3793–3804.
[26] T. Brink, E. Milanese, J.-F. Molinari, Effect of wear particles and roughness on nanoscale friction, Phys. Rev. Mater. 6 (1) (2022) 013606, Publisher: American Physical Society.
[27] C. Varvenne, A. Luque, W.G. Nöhring, W.A. Curtin, Average-atom interatomic potential for random alloys, Phys. Rev. B 93 (2016) 104201.
[28] A.P. Thompson, H.M. Aktulga, R. Berger, D.S. Bolintineanu, W.M. Brown, P.S. Crozier, P.J. in 't Veld, A. Kohlmeyer, S.G. Moore, T.D. Nguyen, R. Shan, M.J. Stevens, J. Tranchida, C. Trott, S.J. Plimpton, LAMMPS - A flexible simulation tool for particle-based materials modeling at the atomic, meso, and continuum scales, Comput. Phys. Comm. 271 (2022) 108171.
[29] V.P. Rajan, D.H. Warner, W.A. Curtin, An interatomic pair potential with tunable intrinsic ductility, Modelling Simulation Mater. Sci. Eng. 24 (2) (2016) 025005, Publisher: IOP Publishing.
[30] A. Stukowski, Visualization and analysis of atomistic simulation data with OVITO-The Open Visualization Tool, Modell. Simul. Mater. Sci. Eng. 18 (1) (2010).
[31] V.V. Bulatov, W. Cai, R. Baran, K. Kang, Geometric aspects of the ideal shear resistance in simple crystal lattices, Phil. Mag. 86 (25–26) (2006) 3847–3859, Publisher: Taylor & Francis _eprint: http://dx.doi.org/10.1080/14786430600643282.
[32] S. Aubry, K. Kang, S. Ryu, W. Cai, Energy barrier for homogeneous dislocation nucleation: Comparing atomistic and continuum models, Scr. Mater. 64 (11) (2011) 1043–1046.
[33] W. Shinoda, M. Shiga, M. Mikami, Rapid estimation of elastic constants by molecular dynamics simulation under constant stress, Phys. Rev. B 69 (13) (2004) 134103, Publisher: American Physical Society.
[34] M. Tuckerman, J. Alejandre, R. López-Rendón, A. Jochim, G. Martyna, A Liouville-Operator derived measure-preserving integrator for molecular dynamics simulations in the isothermal–isobaric ensemble, J. Phys. A: Math. Gen. 39 (19) (2006) 5629–5651, Publisher: IOP Publishing.
[35] T. Brink, J.-F. Molinari, Adhesive wear mechanisms in the presence of weak interfaces: Insights from an amorphous model system, Phys. Rev. Mater. (2019).
[36] S. Pham-Ba, T. Brink, J.-F. Molinari, Adhesive wear and interaction of tangentially loaded micro-contacts, Int. J. Solids Struct. 188–189 (2020) 261–268.
[37] T. Schneider, E. Stoll, Molecular-dynamics study of a three-dimensional one-component model for distortive phase transitions, Phys. Rev. B 17 (3) (1978) 1302–1322, Publisher: American Physical Society.
[38] E.O. Hall, The Deformation and Ageing of Mild Steel: III Discussion of Results, Proc. Phys. Soc. B 64 (9) (1951) 747–753, Publisher: IOP Publishing.
[39] N. Petch, The cleavage strength of polycrystals, J. Iron Steel Inst. 173 (1953).